

The Tell-Tale Heart: Brightness Fluctuations in the Decline of SN 2009ip

J. C. Martin

Barber Observatory, University of Illinois Springfield, Springfield, IL 62704, USA

jmart5@uis.edu

F.-J. Hambusch

Remote Observatory Atacama Desert, Chile

Vereniging Voor Sterrenkunde (VVS), Oude Bleken 12, 2400 Mol, Belgium

R. Margutti

Harvard-Smithsonian Center for Astrophysics, 60 Garden St, Cambridge, MA 02318, USA

T.G. Tan

Perth Exoplanet Survey Telescope, Perth, Australia

I. Curtis

Adelaide, Australia

and

A. Soderberg

Harvard-Smithsonian Center for Astrophysics, 60 Garden St, Cambridge, MA 02318, USA

Received _____; accepted _____

In Preparation, Version 2.0, 140228

ABSTRACT

The supernova impostor SN 2009ip has re-brightened several times since its initial discovery in August 2009. During its last outburst in late September 2012 it reached a peak brightness of $m_v \sim 13.5$ (M_v brighter than -18) causing some to speculate that it had undergone a terminal core-collapse supernova. Relatively high-cadence multi-wavelength photometry of the post-peak decline revealed bumps in brightness infrequently observed in other Type IIn supernovae. These bumps occurred synchronously in all UV and optical bands with amplitudes of 0.1 – 0.4 mag at intervals of 10 – 30 days. Episodic continuum brightening and dimming in the UV and optical with these characteristics is not easily explained within the context of models that have been proposed for the late September 2012 outburst of SN 2009ip. We also present evidence that the post peak fluctuations in brightness occur at regular intervals and raise more questions about their origin.

Subject headings: supernovae: individual (SN 2009ip)

1. Introduction

Maza et al. (2009) first identified SN 2009ip in August 2009 as an under-luminous supernova in NGC 7259 ($z \sim 0.005$, $d \sim 24$ Mpc). Based on further investigation and subsequent eruptions in 2010 and 2011, it was reclassified as a supernova impostor. For additional observational details concerning observed activity of SN 2009ip prior to 2012 see Berger et al. (2009), Li et al. (2009), Smith et al. (2010), Foley et al. (2011).

There were two significant outbursts in 2012: 2012-A and 2012-B. The first on UTC 2012 July 24 (2012-A) (Drake et al. 2012) reached a peak of $m_V \sim 16.8$ and faded. Then a UTC 2012 September 15 spectrum by Smith & Mauerhan (2012) showed signs of a second outburst (2012-B), which they announced as a Type IIn core-collapse supernova. Observations on UTC 2012 September 22 (Margutti et al. 2012) and UTC 2012 September 24 (Martin et al. 2012) detected no change in brightness ($m_V \sim 17.7$). But soon after that, SN 2009ip brightened more than three magnitudes in less than 50 hours (Brimacombe 2012; Margutti et al. 2012; Prieto et al. 2013).

The 2012-B outburst was the brightest observed yet for SN 2009ip, reaching a peak brightness of $m_V \sim 13.5$ ($M_V < -18$). Consequently, several authors have analyzed the 2012-B outburst and considered evidence that it was a terminal core-collapse supernova explosion. Some have concluded that it was a terminal explosion (Prieto et al. 2013; Mauerhan et al. 2013; Smith et al. 2013). Others have questioned if it was a core-collapse supernova (Pastorello et al. 2013; Fraser et al. 2013; Soker & Kashi 2013; Margutti et al. 2013).

Fraser et al. (2013) and Margutti et al. (2013) noted brightness fluctuations in the decline of the 2012-B outburst that are not present in most other well sampled Type IIn light curves (Kiewe et al. 2012; Taddia et al. 2013). Similar fluctuations maybe present in a subset of Type IIn light curves including SN 1994W (Sollerman et al. 1998), SN 2005la

(Pastorello et al. 2008), SN 2005ip (Smith et al. 2009) and SN 2010mc (Ofek et al. 2013) but they have not received detailed attention.

The observed bumps in brightness were a change of several percent or more relative to the total flux. To our knowledge, there is no record of comparable variations in flux of the major features in the emission spectrum that can to an order of magnitude account for these bumps (Mauerhan et al. 2013; Fraser et al. 2013; Margutti et al. 2013). We have not conducted an independent search of the published spectra and the sampling may be too sparse to detect a clear correlation between relatively small changes in the emission features and any of the bumps. While there is no obvious correlation with large scale changes in the emission features, the bumps are clearly present in the derived temperature and bolometric luminosity of blackbody continuum fits to the photometry (Margutti et al. 2013). This may imply that the bumps are primarily driven by changes in the continuum brightness.

Bright emission lines in the spectra of Type II_n supernovae may vary as the post-break-out shock interacts with density variations in the circumstellar medium (Chugai & Danziger 1994; Fransson et al. 2002). These occur in an optically thin regime that almost exclusively produces radio and X-ray emission, without significant visual continuum brightening. (Chevalier & Fransson 1994; Nymark et al. 2006; Dwarkadas & Gruszko 2012; Chandra et al. 2012). When the supernova is embedded in an optically thick envelope, the radiation produced by the shock is processed before reaching the observer (Falk & Arnett 1977; Chevalier & Irwin 2011; Balberg & Loeb 2011). Under these circumstances, high energy photons produced in shock interactions may emerge as optical continuum after passing through material of sufficient optical depth (Murase et al. 2011; Chevalier & Irwin 2012; Svirski et al. 2012).

The most basic models assume that energy uniformly diffuses outward through successive layers until it streams freely through space to the observer. In reality, the

structure of the circumstellar environment may contain asymmetric clumps or large structures that break spherical or bipolar symmetry. Computer simulations show that geometry, density gradient, and other qualities of the circumstellar envelope may significantly influence the observed bolometric lightcurve for the supernova (van Marle et al. 2010; Woosley et al. 2007; Smith & McCray 2007; Moriya et al. 2013). However it is still uncertain how asymmetric or more complicated geometry may affect the observed light curve and spectrum. The term “photosphere” can be confusing because it commonly evokes a uniform opaque surface or shell completely enclosing a source of energy diffusing through it. Following the lead of Margutti et al. (2013) we attempt to avoid this confusion by referring to the source of optical and UV continuum photons in the SN 2009ip spectrum as the “continuum emitting region” independent of model, geometry or source of heating.

Mauerhan et al. (2013) propose a scenario for SN 2009ip where the 2012-A event was a terminal core-collapse and the interaction of that shock wave with an already existing dense circumstellar envelope produced the 2012-B peak brightness. They conclude based on spectra of high velocity ($> 8000 \text{ km s}^{-1}$) ejecta that SN 2009ip underwent a terminal core-collapse supernova explosion at the time of the 2012-A outburst. Prieto et al. (2013) agree but Pastorello et al. (2008) question if high velocity ejecta alone is “conclusive proof” of a terminal core-collapse. Margutti et al. (2013) demonstrated that the expansion of the photosphere during the 2012-B event is too fast to have originated in the 2012-A event and calculate the total radiated energy of the 2012-B eruption to be 3.2×10^{49} ergs. Both Fraser et al. (2013) and Margutti et al. (2013) also found *no* evidence of supernova nucleosynthesis in late-time spectra ($t > +150$ days). Smith et al. (2013) argue that the radiated energy could account for 5% or less of the total energy and speculate about alternatives for the absence of oxygen rich material in the late-time spectra.

Considering alternative scenarios, the bumps in the light curve could be caused by

heating *in addition* to the main shock-interaction. The additional heating may come from a surviving progenitor, neutron star or blackhole produced in a core-collapse supernova. Or one referee suggested the opposite: that the dominate mechanism for the late-time light curve may not be interaction and the fluctuations themselves are powered by the addition of power from interaction with an inhomogeneous CSM. A detailed computational analysis of these alternatives is outside the scope of this paper.

Slow moving ejecta may also interact with the circumstellar medium at later times (after peak brightness) adding to the observed brightness. Levesque et al. (2014) postulate that the 2012-B brightening was due to the illumination of the inner rim of a dense equatorial disk through interaction with fast moving ejecta. They argue that the Balmer line ratios imply a high density over a relatively small surface area so that a disk geometry is favored over shockwave interaction with spherical shells. This presents an interesting alternative that could be consistent with the bumps in the decline. The continuum emitting region situated in the disk could be reheated in episodes throughout the decline when slow moving or later ejected fast moving material interacts with the inner rim *after* the initial shock wave passed. Smith et al. (2013) find no spectroscopic evidence of slower moving ejecta interacting at later times but this does not rule out faster ejecta originating from the source after the peak brightness.

Soker & Kashi (2013) and Kashi et al. (2013) provide a model for the 2012-B eruption involving a merger burst in a binary star system. They focus on the two largest fluctuations in the decline at $t= +30$ and $t= +60$ days. In their model those peaks mark interactions between stars in a binary system during periastron passage. The excreted material impacts slower moving optically thick material, heating it and producing observable continuum. Material excreted from the binary continues to impact and heat the continuum emitting region throughout the decline at regular intervals associated with the frequency of the

binary orbit.

This paper extracts and attempts to characterize the brightness fluctuations in the light curve. It is organized into three sections. In Section 2 we describe the photometry and how it was measured. In Section 3 we analyze the data and characterize the fluctuations. A discussion and conclusions are provided in Section 4.

All uncertainties given in this paper are one-sigma unless otherwise noted. We use U, B, V, Rc, and Ic to refer to standard Johnson-Cousins filters. The Swift/UVOT filters are referred to with lowercase b, u, w1, m1, and w2. Magnitudes are zero-pointed to Vega on the Johnson System. Time is referred to in the manner adopted by Margutti et al. (2013) where t is given in days and $t = 0$ is MJD 56203 (October 3, 2012 UT) corresponding with the peak UV brightness. Where observed flux is converted to luminosity we make the same assumptions as Margutti et al. (2013) and Foley et al. (2011): a distance of 24 Mpc and a Milky Way extinction $E(B - V) = 0.019$ (Schlegel et al. 1998) with no extinction in the host galaxy.

2. Observations

2.1. Ground-Based Optical Measurements

Images of SN 2009ip were obtained in the V, Rc and Ic bands using four telescopes: the University of Illinois Springfield (UIS) Barber Observatory 20-inch telescope with an Apogee U42 CCD camera using a back-illuminated E2V CCD42-40 chip (Pleasant Plains, IL), a 16-inch f/6.8 reflecting telescope with a Finger Lakes Instruments (FLI) CCD camera using a Kodak 16803 chip operated by Franz-Josef Hamsch at the Remote Observatory

Atacama Desert (Hambusch 2012), the Perth Exoplanet Survey Telescope (PEST)¹ a 12-inch Meade schmidt-cassegrain telescope (SCT) with an Artemis 285 CCD camera using a Sony ICX285AL chip operated by TG Tan (Perth, Australia), and a C11 SCT with a ATIK 320E mono CCD camera using a Sony ICX274 chip operated by Ivan Curtis (Adelaide, Australia). The Barber Observatory imaged all bands with 600-second exposures. Hambusch obtained 240-second exposures in V and Ic bands in pairs. Curtis and Tan took a series of high cadence 120-second R-band images over 2 – 5 hours each night they observed. The photometry from individual images in the high cadence series were averaged together as single magnitude reported for the night.

The brightness was measured using circular apertures adjusted for seeing conditions and sky background annuli around each aperture. The aperture size and sky annuli were held constant when reducing a continuous series of images from a single telescope on the same night. Twenty comparison stars within 10 arc minutes of the target were selected from the AAVSO Photometric All-Sky Survey ² (Henden et al. 2012). The Barber, Hambusch, and Tan images were reduced using an unweighted average of results from all the comparison stars. The Curtis images covered a smaller field and were reduced using an unweighted average of a sub-set of these comparisons. A small correction was applied to Curtis’ photometry to account for any systematic offsets introduced by the subset of comparisons used. When pairs of images were taken by Hambusch at roughly the same time, photometry was measured from the individual images and then averaged together. Statistical errors in the photometry for individual images was typically 0.05 magnitudes or less. Photometry taken by different telescopes on the same night compare favorably with each other within the statistical errors. Finally, the photometry was corrected to the system of Pastorello

¹http://www.angelfire.com/space2/tgtan/PEST_description.pdf

²<http://www.aavso.org/apass>

et al. (2013) using the corrections of: $dV = +0.063$, $dRc = +0.046$ and $dIc = +0.023$ (Pastorello, personal communication). There were no additional transformations for color or other factors applied to the measured magnitudes.

The Rc and Ic magnitudes are published in their entirety in Margutti et al. (2013). The V magnitudes prior to $t = +10$ days were previously published in Pastorello et al. (2013). The later V magnitudes are in Table 1.

2.2. Swift UVOT Measurements

SWIFT UVOT data in the b, u, w1, m1, and w2 bands are taken from Margutti et al. (2013) where they are described in detail. The data were analyzed following the prescription of Brown et al. (2009) with apertures optimized to maximize signal-to-noise and limit contamination from nearby stars. The magnitudes are on the UVOT photometric system (Poole et al. 2008) and revised to the Vega zero points of Breeveld et al. (2011). The b and u data are converted to equivalent Johnson U and B magnitudes by Margutti et al. (2013). They note this is a minor correction that is *not* responsible for the bumps in the light curve.

3. Analysis

3.1. Optical Peak and Decline

Our measurements begin on $t = -9.16$ days very near to the start of the rise in brightness toward the 2012-B peak (Pastorello et al. 2013). The supernova brightness increased about 4 magnitudes in 12 days in V, Rc, and Ic, reaching a peak $V = 13.80 \pm 0.05$ on $t = +3$ days (MJD 56206.04), which is consistent with observations reported by

Prieto et al. (2013).

The post peak bolometric flux of most Type IIn supernovae are modeled by a power law function of flux with respect to time (Svirski et al. 2012; Moriya et al. 2013). Bolometric magnitude is directly proportional log of bolometric flux. Therefore, an power law in flux-time is linear when transformed to a function of bolometric magnitude with respect to the logarithm of time. For a sample whose duration spans a few decades of time, bolometric magnitude is nearly linear with respect to time.

The dominant trend in the decline in magnitude from the peak is almost linear with respect to time within the first 60 days (see Section 3.2). Fitting a purely linear function we obtained slopes of: 0.060 ± 0.005 mag/day in V, 0.050 ± 0.001 mag/day in Rc and 0.094 ± 0.026 mag/day in Ic. The slopes differ due to different bolometric corrections in each filter. The rapid rise and rates of decline, within 60 days of the peak are consistent with other Type IIn light curves (Kiewe et al. 2012; Taddia et al. 2013).

3.2. Removal of the Underlying Trend

The observed brightness after the peak contains significant fluctuations superimposed on a downward trend which are easily identified in all eight bands. Each telescope observed these fluctuations independently, eliminating the concern that it could be an effect attributable to a single telescope or observing location. Margutti et al. (2013) notes the regular placement of “peaks” in the general trend and that an analysis of the Rc-band photometry prior to the 2012-B event reveals some power in periods between 20 - 40 days.

To analyze this structure, we subtracted the peak and linear decline from data in each band. The best models of the trend after the peak are power law functions of bolometric flux with respect to time (eg. Svirski et al. (2012); Moriya et al. (2013)) which are linearized

as functions of bolometric magnitude with respect to the logarithm of time. The magnitudes in this work are not bolometric and the bolometric correction is likely to be variable with respect to time (Margutti et al. 2013). A more complicated model (i.e. the sum of two power laws in flux-time) is difficult to linearize and fit to the data using a least squares method. With these caveats in mind, a second degree polynomial of magnitude with respect to time is a reasonable low order approximation to the physical models.

Margutti et al. (2013) found significant transitions in the thermal continuum at $t = +16$ and $t = +70$ days. The light curves in each band visibly change character at $t \sim +10$ days and $t \sim +70 - 75$ days. To accomodate this, our fit employed two second degree polynomials bracketed by these transitions (see example in Figure 1). The first was fit to the data around the peak for $-8 < t < +10$ days. The second was fit to the decline between $+10 > t > +75$ days. The coefficients for these fits are recorded in Table 2. The small χ^2 for these fits (Table 2) indicate that there is a high probability they are consistent with the trend in the data.

In order to compare with the physical models, we performed fits to the light curves in the interval of $+10 > t > +75$ days to a linear function of magnitude with respect to the logarithm of time. The χ^2 for all but one those fits (Table 2) demonstrate that they do not fit the data as well as the second degree polynomial. In all cases, the function with respect to $\text{Log}(t)$ is a poor fit to the data at the extreme ends of the range (illustrated in Figure 1). The exception is the data for the w2 filter which is fit slightly better by the linear function with respect to $\text{Log}(t)$ than the second degree polynomial.

We acknowledge that there is a unquantifiable (but likely small) risk that the second order polynomial slightly over-subtracts the underlying trend. A systematic influence of this type should increase red (Brownian) noise and reduce the significance of the bumps and dips. If this effect is present there is also some risk that the relative heights of the

peaks in different band-passes could be effected. But it should have negligible effect on the spacing and frequency of the peaks.

The use of a relatively low order polynomial also risks under-subtraction of the underlying trend. As with the risk of over-subtraction this may have increased the Brownian noise and possibly over emphasized the bumps in the decline. To test this, similar fits were made to Type IIIn supernova light curves from Taddia et al. (2013). Subtraction of the fits generated using the same method from those light curves revealed no significant fluctuations at the one sigma level or greater relative to the quoted measurement errors in the individual data points. If present, under-subtraction could also influence the relative heights of the peaks in each band-pass but should have a negligible effect on the spacing and frequency of the peaks.

3.3. Brightness Fluctuations in the Decline

The data with the modeled trends subtracted are plotted in Figure 2. The trend-subtracted data contains a series of peaks and troughs that have amplitude of 0.10 to 0.40 magnitudes in each band. There are three larger dips followed by rises at approximately $t = +5 - +15$ days, $t = +20 - +40$ days, and $t = +45 - +65$ days. These fluctuations roughly match transition points in the evolution of the thermal continuum as modeled by (Margutti et al. 2013) (see their Figure 8).

We detected no significant variability with a period of less than one day. Tan and Curtis made high cadence observations with a series of 120 second exposures spanning 2 – 5 hours over 26 separate nights (in three circumstances both observing simultaneously on the same night). Those observations revealed no fluctuations in brightness of 2009ip on the time-scale of hours at or above the one-sigma noise level.

Figure 3 shows how the fluctuations evolve relative to each band over time. All the bands start out fluctuating in phase and at roughly the same amplitude. The bump at $t \sim +10$ days is the first point where the bands separate, with the shorter wavelengths peaking at a higher amplitude. At that point the UV bands (w1, w2, and m2) fall out of phase with the optical bands (Ic, Rc, V, B, and U). The UV leads the optical into the dip at $t \sim +25$ days and lags the optical by about one day coming out of the dip. This lag was noted by Fraser et al. (2013) but in contrast to their findings, we observe no lag in U relative to V and the amplitude measured from the low point at $t \sim +25$ days to the peak at $t \sim +32$ days differs significantly depending on wavelength. At $t \sim +45$ days the U and B bands fall out of phase with the V band, lagging that band by about 1 day and matching phase with the UV fluctuations. The peak at $t \sim +60$ days is brightest in the U band and slightly fainter in the B band, with the V and UV bands having roughly the same lower amplitude.

These fluctuations are likely to be driven by continuum changes rather than by variations in the emission lines. A change in flux of 0.1 magnitude in the filters used equals a change of $500\text{\AA} - 2000\text{\AA}$ or more in equivalent width. Adopting the distance modulus and bolometric correction for SN 2009ip used by Margutti et al. (2013), the peaks represent an increase in total luminosity of approximately $10^{42} \text{ erg s}^{-1}$ and the integrated energy of a single peak (from the trend subtracted data) is approximately 10^{47} ergs. No changes of this magnitude, on the timescale of these fluctuations, were reported in the spectrum of SN 2009ip (Mauerhan et al. 2013; Pastorello et al. 2013; Margutti et al. 2013).

A peak or dip in brightness driven by a change in size of the continuum emitting region should affect the brightness in all filters equally. But Figure 3 reveals *relative* differences in color in each of the major peaks. A relative heating of the continuum emitting region should cause shorter wavelengths to brighten relative to longer wavelengths while a relative cooling should cause longer wavelength to brighten relative to shorter wavelengths.

In order to properly interpret the data, recall that we have subtracted the underlying trend so that differences in brightness between bands measure relative color. An increase in brightness in shorter wavelength bands relative to longer wavelengths reveal the color becoming bluer, which can be interpreted as a wavelength dependent change in opacity (i.e. line blanketing) or relative heating. Line blanketing can have the effect of reducing through increased opacity and enhancing through re-emission the brightness in specific filters leaving others unaffected. Relative heating or cooling will proportionally effect all the filters according to the shift in peak of the blackbody continuum. The analysis in Margutti et al. (2013) determined that while these fluctuations were occurring the continuum emitting region was expanding and cooling. In the context of a black body continuum, a local peak in brightness can represent heating relative to the subtracted trend in declining temperature but the absolute temperature of each subsequent peak declines as time progresses. Two peaks may have the same amplitude, revealing comparable heating, but the later one has a cooler absolute temperature.

For the first peak at $t \sim +8 - +15$ days and the following dip between $t \sim +20 - +30$ days the UV bands have a greater amplitude than the visual. This could correspond to heating of the continuum emitting region to produce the peak and then cooling to produce the dip. According to Margutti et al. (2013) this peak occurs when the effective temperature of the thermal continuum is between 15,000 K to 11,000 K.

The second major peak between $t \sim +30 - +40$ is different than the first. All bands reach the same amplitude, but the UV bands lag the optical bands by ~ 1 day. This does not fit the expectation for a change driven by the shift in wavelength peak of a blackbody continuum. The lag in UV brightness is better understood in the context of line blanketing which simultaneously reduces brightness though increased opacity in one wavelength range and raises the brightness through re-emission in another. Rising out of the minimum,

significant line blanketing could simultaneously lower the UV flux and enhance the visual bands through re-emission. This roughly corresponds to the explanation put forward by Fraser et al. (2013) for the lag between bands in this peak. After the peak the ionization of the continuum emitting region changes eliminating the line blanketing and causing the UV to be brighter throughout the decline. According to Margutti et al. (2013) this peak occurs when the effective temperature of the thermal continuum is between 9500 K to 8000 K.

The third major peak shows a lag in both the UV and the blue optical bands. This peak is brightest in the U and B bands and less prominent in the longer wavelength optical and UV. The presence of the Balmer continuum/decrement in the U and B bands along with their divergent behavior relative to the other bands alludes to a transition in the ionization state of hydrogen. According to Margutti et al. (2013) this peak occurs when the effective temperature of the thermal continuum is between 6500 K to 5500 K. There is probably some combination of line blanketing and temperature change at work in this peak which occurs at a lower absolute temperature than the first two peaks. Spectra from this time hint at an increase in structure at wavelengths shorter than 4000\AA along with a significant increase in Balmer (Margutti et al. 2013) and Paschen (Fraser et al. 2013) emission.

3.4. Power Spectrum Analysis of the Fluctuations

The placement of the three major peaks and several smaller peaks imply a possible regularity in the fluctuations. Kashi et al. (2013) note the major bumps occur roughly 24 days apart and attributes this to binary interaction. The behavior prior to $t = +8$ days is also very regular. It should also be noted that the fluctuations after the eruption are consistent with those detected prior to the eruption as part of a binary or single star model. Flickering (fluctuations on the order of 3 magnitudes in brightness over ~ 16 days) was

observed in earlier eruptions of SN 2009ip (Smith et al. 2010; Foley et al. 2011). Margutti et al. (2013) also found periods of fluctuation between 20 - 40 days in the R-band prior to the 2012-A eruption.

There is already evidence for regularity in the fluctuations. The power spectrum analysis that follows is performed to corroborate and quantify what is already supported by that evidence. Without corroborating evidence, the results of our power spectrum analysis should be considered with caution. One objection may be that the data set is short and spans an insufficient length of time to yield meaningful results. To mitigate this concern we ignore the lowest frequencies in the power spectrum which correspond to periods more than one third the total time spanned by the data. Another concern is Brownian (red) noise. See the caveats and concerns outlined at the end of Section 3.2. The process to subtract the underlying trend is certain to introduce noise heavily weighted toward low frequencies. To answer those concerns we have applied a tested and peer-reviewed algorithm to estimate the confidence level of the peaks relative to Brownian noise (see below). There may still be doubts about the validity of the power spectrum analysis results on their own, but to the extent that they corroborate other observations they are compelling.

We analyzed the fluctuations using a date compensated discrete Fourier transform (DCDFT) (Ferraz-Mello 1981) in the AAVSO software package VStar³. The analysis was performed on two different samples of the data (Figure 4). The power spectrum derived from all the data shows a relatively narrow peak at a frequency of 0.085 day^{-1} (period ~ 12 -days), a small bump at a frequency of 0.061 day^{-1} (period ~ 16 -days), and a much broader peak at frequency of 0.042 day^{-1} (period ~ 24 -days). The same analysis, excluding the data during the transition between $t = +20 - +40$ days yields a power spectrum with peaks in power at roughly the same frequencies. The 12 and 16 day periods are likely

³<http://www.aavso.org/vstar-overview>

harmonics ($1/2$ and $2/3$) of the 24 day period. The power distributed at frequencies between 0.11 and 0.17 are also likely to be sub harmonics.

The process by which the underlying trend was subtracted is likely to introduce Brownian noise into the data. This is evident in Figure 4 as a continuous decrease in spectral amplitude with increasing frequency. Similar noise dominates plaeoclimate data (Hasselmann 1976) and can be modelled using a first-order autoregressive (AR1) process. Schulz & Mudelsee (2002) provide an algorithm to model this noise in an unevenly spaced time series and simulate confidence levels in order to determine the significance of peaks in the power spectrum. Figure 5 shows the results of applying their code to our data using $N = 10^4$ for the Monte-Carlo simulation. Many of the peaks in the power spectrum fall between the level of simulated AR1-type noise and the 80% confidence level. The peak at 0.085 day^{-1} (period ~ 12 -days) is just above the 80% confidence limit and the peak at 0.042 day^{-1} (period ~ 24 -days) has a confidence between 95% – 99%. Peaks above a 95% confidence level have less than a 5% chance of being a false alarm. This simulation implies that at least one of the observed peaks in the power spectrum are *not* a product of AR1-type Brownian noise.

4. Discussion

The light curve for the 2012-B outburst was exceptionally well-sampled raising the possibility that these fluctuations are common in the light-curves of Type IIn and have only been uncovered as a result of greater scrutiny. Other well-sampled Type IIn light curves (Kiewe et al. 2012; Taddia et al. 2013) do *not* have similar brightness fluctuations in their decline. While the 2012-B eruption of SN 2009ip clearly meets the spectroscopic definition of a Type IIn (Smith & Mauerhan 2012; Mauerhan et al. 2013; Pastorello et al. 2013; Fraser et al. 2013; Margutti et al. 2013; Smith et al. 2013), and the peak absolute magnitude is

consistent with a terminal explosion (Mauerhan et al. 2013; Pastorello et al. 2013; Fraser et al. 2013; Margutti et al. 2013), the bumpy decline of SN 2009ip is not prevalent among other Type IIns. Fraser et al. (2013) note that the fluctuations in SN 2009ip share some characteristics with SN 2005la which Pastorello et al. (2008) classified type-Ibn sharing some characteristics of “classical” Type IIn events. The light curves of a few other Type IIn events (i.e SN 1994W (Sollerman et al. 1998), SN 2005la (Pastorello et al. 2008), SN 2005ip (Smith et al. 2009) and SN 2010mc (Ofek et al. 2013)) appear to have similar fluctuations however they have never been discussed in length.

Interaction of the expanding supernova shock-wave with circumstellar material or other related mechanisms could cause fluctuations in brightness after the peak of the light curve. Many of the models which have proposed for the 2012-B eruption of SN 2009ip employ this mechanism (see Section 1). However, none those models clearly and quantitatively address the observed fluctuations. Some permutation of those models may be capable of reproducing the fluctuations under tuned conditions. It remains to be proven if those conditions are reasonable or not. Further exploration along those lines is outside the scope of this paper and best left to others with access to the appropriate expertise and modeling codes.

Type-Ia supernovae sometimes show a secondary peak powered by continuum brightening in the red and infrared spectral region of the spectrum (Elias et al. 1981). The origin of the second Ia peak is reprocessed radiation driven by recombination and subsequent line blanketing in the ultraviolet part of the spectrum (Kasen 2006). We note a correlation between a change in ionization state/opacity in the thermal continuum blackbody fits of Margutti et al. (2013) and the second and third major peaks (Section 3.3). Fraser et al. (2013) postulate that scattering could play a role in the dips and peaks. However, unlike the secondary peaks in type-Ia, the fluctuations in SN 2009ips decline were

less prominent in the red and NIR part of the spectrum (Margutti et al. 2013).

Under specially constructed circumstances the light curve fluctuations can be modeled with light echoes. It is possible to contrive an environment where the bumps are reproduced by shells of the proper shape, orientation, and solid angle to introduce the bumps as scattered light echos of the primary eruption. The periodic nature of the bumps could be explained by nested shells expelled during periodic episodes of mass loss from the progenitor. It is not uncommon to find nested shells at some regular frequency around stars at late stages in their evolution. However, the albedo for the scattering and/or the effective solid angle subtended by these structures would have to be exceptionally high in order to produce echos on the order of several percent of the brightness. The geometric tolerances are further constrained by the delays of the major peaks. Delays of +10, +30 and +60 days from the peak would require distances of 870 AU, 2600 AU, and 5200 AU respectively between the progenitor and the near-point on the semi-major axis of properly oriented partial ellipsoidal shells. The model would also have to successfully explain the key differences in brightness as a function of filter in each of the successive peaks described in section 3.3. We cannot rule out light echos as a possible explanation for the bumps but it appears to require a very complicated model to satisfy all our observations.

Soker & Kashi (2013) and Kashi et al. (2013) model the fluctuations as interactions between shells of material excreted from a binary system embedded inside a slower moving cocoon of material. The power spectrum (Figure 4) contains frequency peaks and harmonics that loosely evoke the rhythm of a pulsating star. Following the prescription of Eddington (1926) we computed the mean density of a star ($\bar{\rho}$) undergoing adiabatic radial pulsation at certain frequencies (f) using the relation:

$$\bar{\rho} = \pi \left[\frac{f}{(\gamma - \frac{4}{3})G} \right]^2$$

Assuming the effective ratio of specific heats for the pressure-density relation is $\gamma = \frac{5}{3}$

and $G = 6.67 \times 10^{-8} \text{cm}^3 \text{g}^{-1} \text{s}^{-1}$. The resulting mean stellar density, $\log(\bar{\rho}/\bar{\rho}_{\odot}) \sim -4.0$ to -4.6 for frequencies of 12 to 24 days, corresponds to an A-type super-giant with a surface temperature between 10,000 K and 8000 K and an absolute visual magnitude between -8.5 and -9.0 (Lang 1992). These are consistent with the parameters for the proposed progenitor of SN 2009ip positioned near the Humphrey-Davidson limit on the HR-diagram (Smith et al. 2010; Foley et al. 2011). This is an interesting coincidence and we acknowledge that there are many additional details that must be considered to incorporate this information into a viable model including stellar pulsation.

The models for Type II_n SNe have encountered a number of paradoxes in SN 2009ip. Although their nature remains uncertain, the bumps in the decline from the 2012-B eruption appear to be real and there is further evidence that they are periodic. This phenomena deserves further study. Do these fluctuations in some Type II_n have a common origin? Perhaps they can provide clues as to the nature of this class of supernovae.

J.C. Martin's work is supported by the National Science Foundation grant AST1108890. R. Margutti thanks the Swift team for their excellent support in scheduling the observations. We wish also to thank Jim O'Brien and Jennifer Hubbell-Thomas for assisting with observations included in this publication and the patrons of the UIS Barber Observatory for their financial support of the Henry R. Barber endowment for Astronomy at the University of Illinois Springfield. Thanks to R.M. Humphreys and K. Davidson who provided several constructive comments. Thank you also to the anonymous referee whose thoughtful criticism greatly improved this paper. J.C. Martin makes a heartfelt acknowledgment of contributions by George W. Collins III made posthumously through notations recorded in the margin of Martin's copy of Eddington (1926).

REFERENCES

- Balberg, S., & Loeb, A. 2011, MNRAS, 414, 1715
- Berger, E., Foley, R., & Ivans, I. 2009, The Astronomer's Telegram, 2184, 1
- Breeveld, A. A., Landsman, W., Holland, S. T., et al. 2011, American Institute of Physics Conference Series, 1358, 373
- Brimacombe, J. 2012, The Astronomer's Telegram, 4423, 1
- Brown, P. J., Holland, S. T., Immler, S., et al. 2009, AJ, 137, 4517
- Chandra, P., Chevalier, R. A., Chugai, N., et al. 2012, ApJ, 755, 110
- Chevalier, R. A., & Fransson, C. 1994, ApJ, 420, 268
- Chevalier, R. A., & Irwin, C. M. 2012, ApJ, 747, L17
- Chevalier, R. A., & Irwin, C. M. 2011, ApJ, 729, L6
- Chugai, N. N., & Danziger, I. J. 1994, MNRAS, 268, 173
- Drake, A. J., Howerton, S., McNaught, R., et al. 2012, The Astronomer's Telegram, 4334, 1
- Dwarkadas, V. V., & Gruszko, J. 2012, MNRAS, 419, 1515
- Eddington, A. S. 1926, The Internal Constitution of the Stars, Cambridge: Cambridge University Press, 1926. ISBN 9780521337083.,
- Elias, J. H., Frogel, J. A., Hackwell, J. A., & Persson, S. E. 1981, ApJ, 251, L13
- Falk, S. W., & Arnett, W. D. 1977, ApJS, 33, 515
- Ferraz-Mello, S. 1981, AJ, 86, 619

- Fraser, M., Inserra, C., Jerkstrand, A., et al. 2013, MNRAS, 433, 1312
- Foley, R. J., Berger, E., Fox, O., et al. 2011, ApJ, 732, 32
- Fransson, C., Chevalier, R. A., Filippenko, A. V., et al. 2002, ApJ, 572, 350
- Hambusch, F.-J. 2012, Journal of the American Association of Variable Star Observers (JAAVSO), 40, 1003
- Hasselmann, K. 1976, Stochastic climate models: Part I. Theory. Tellus 28(6), 473-485.
- Henden, A. A., Levine, S. E., Terrell, D., Smith, T. C., & Welch, D. 2012, Journal of the American Association of Variable Star Observers (JAAVSO), 40, 430
- Kashi, A., Soker, N., & Moskovitz, N. 2013, MNRAS, 436, 2484
- Kasen, D. 2006, ApJ, 649, 939
- Kiewe, M., Gal-Yam, A., Arcavi, I., et al. 2012, ApJ, 744, 10
- Lang, K. R. 1992, Astrophysical Data I. Planets and Stars, X, 937 pp. 33 figs.. Springer-Verlag Berlin Heidelberg New York.
- Levesque, E. M., Stringfellow, G. S., Ginsburg, A. G., Bally, J., & Keeney, B. A. 2014, AJ, 147, 23
- Li, W., Smith, N., Miller, A. A., & Filippenko, A. V. 2009, The Astronomer's Telegram, 2212, 1
- Margutti, R., Soderberg, A., & Milisavljevic, D. 2012, The Astronomer's Telegram, 4414, 1
- Margutti, R., Soderberg, A., Chornock, R., & Foley, R. 2012, The Astronomer's Telegram, 4425, 1
- Margutti, R., Milisavljevic, D., Soderberg, A. M., et al. 2013, arXiv:1306.0038

- Martin, J. C., O'Brien, J., & Hubbell-Thomas, J. 2012, *The Astronomer's Telegram*, 4416, 1
- Mauerhan, J. C., Smith, N., Filippenko, A. V., et al. 2013, *MNRAS*, 430, 1801
- Maza, J., Hamuy, M., Antezana, R., et al. 2009, *Central Bureau Electronic Telegrams*, 1928, 1
- Miller, A. A., Li, W., Nugent, P. E., et al. 2009, *The Astronomer's Telegram*, 2183, 1
- Moriya, T. J., Maeda, K., Taddia, F., et al. 2013, *MNRAS*, 435, 1520
- Murase, K., Thompson, T. A., Lacki, B. C., & Beacom, J. F. 2011, *Phys. Rev. D*, 84, 043003
- Nymark, T. K., Fransson, C., & Kozma, C. 2006, *A&A*, 449, 171
- Ofek, E. O., Sullivan, M., Cenko, S. B., et al. 2013, *Nature*, 494, 65
- Pastorello, A., Quimby, R. M., Smartt, S. J., et al. 2008, *MNRAS*, 389, 131
- Pastorello, A., Cappellaro, E., Inserra, C., et al. 2013, *ApJ*, 767, 1
- Poole, T. S., Breeveld, A. A., Page, M. J., et al. 2008, *MNRAS*, 383, 627
- Prieto, J. L., Brimacombe, J., Drake, A. J., & Howerton, S. 2013, *ApJ*, 763, L27
- Schultz, M., & Mudelsee, M. 2002, *Computers & Geosciences*, 28, 421
- Schlegel, D. J., Finkbeiner, D. P., & Davis, M. 1998, *ApJ*, 500, 525
- Soker, N., & Kashi, A. 2013, *ApJ*, 764, L6
- Sollerman, J., Cumming, R. J., & Lundqvist, P. 1998, *ApJ*, 493, 933
- Smith, N., Mauerhan, J. C., & Prieto, J. L. 2014, *MNRAS*, 438, 1191

- Smith, N., Mauerhan, J. C., & Prieto, J. L. 2014, MNRAS, 438, 1191
- Smith, N., & Mauerhan, J. 2012, The Astronomer’s Telegram, 4412, 1
- Smith, N., & McCray, R. 2007, ApJ, 671, L17
- Smith, N., Miller, A., Li, W., et al. 2010, AJ, 139, 1451
- Smith, N., Silverman, J. M., Chornock, R., et al. 2009, ApJ, 695, 1334
- Svirski, G., Nakar, E., & Sari, R. 2012, ApJ, 759, 108
- Taddia, F., Stritzinger, M. D., Sollerman, J., et al. 2013, A&A, 555, A10
- van Marle, A. J., Smith, N., Owocki, S. P., & van Veelen, B. 2010, MNRAS, 407, 2305
- Woosley, S. E., Blinnikov, S., & Heger, A. 2007, Nature, 450, 390

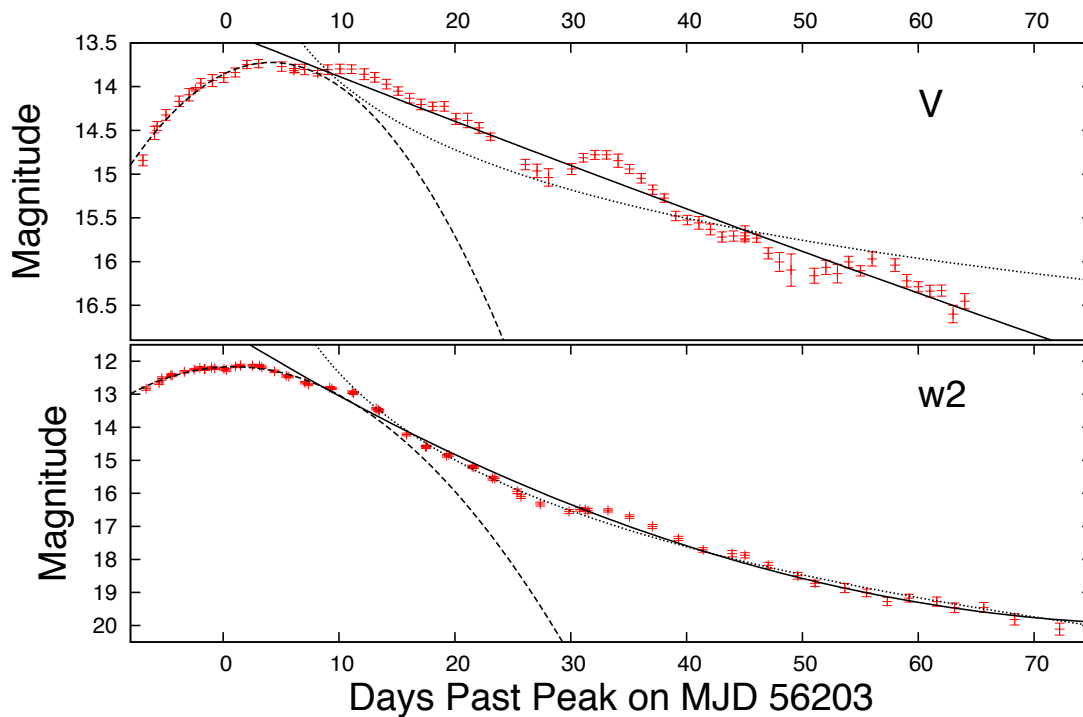


Fig. 1.— An example of how the fits (see Table 2) were made to the V-band data (top panel) and w2 data (bottom panel). The y-error bars are one sigma statistical errors. The solid line and the dashed line are the second order polynomial fit between $+10 > t > +75$ days and $-8 < t < +10$ days respectively. The dotted line is the attempt at fitting a linear function with respect to $\text{Log}(t)$ between $+10 > t > +75$ days. The fit trends were subtracted from the data to produce Figure 2.

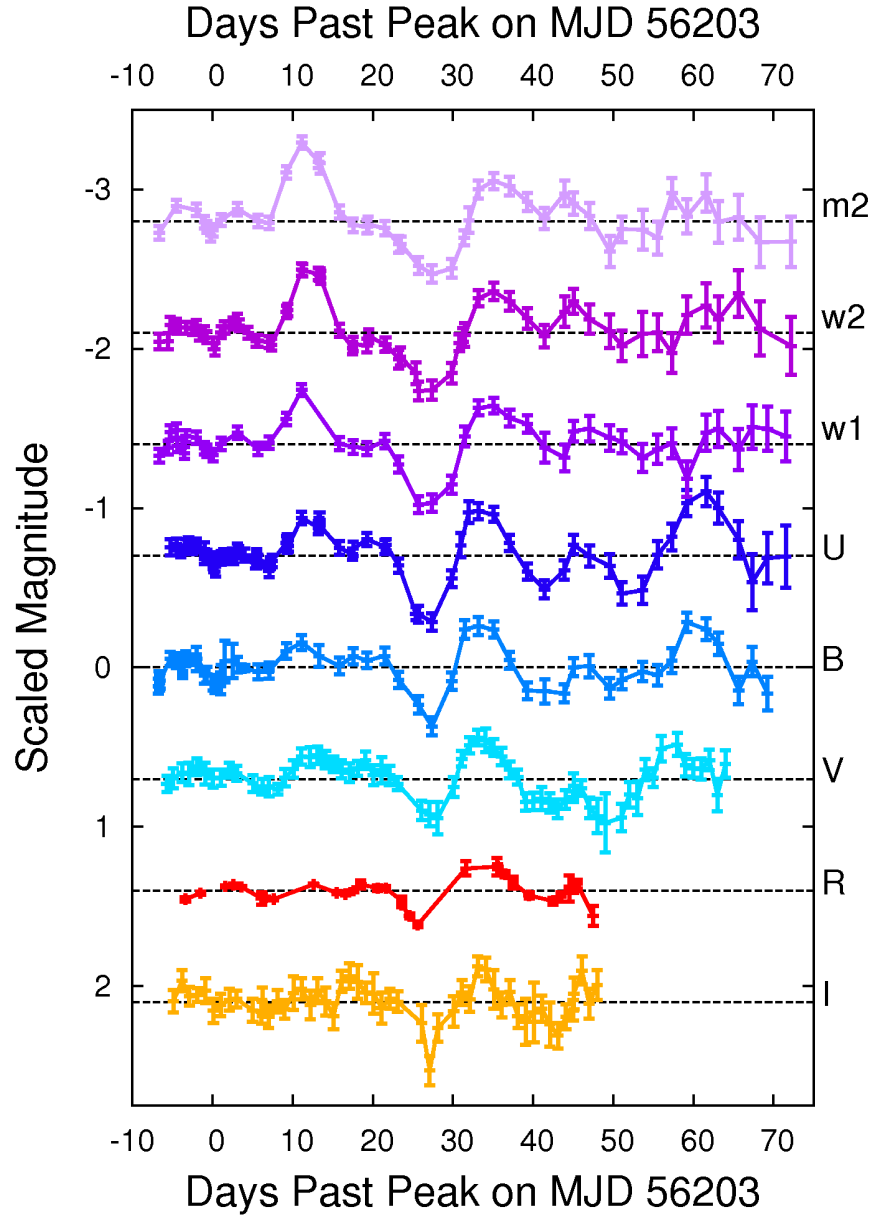


Fig. 2.— Brightness vs time during 2012-B outburst with the fit to the decline subtracted. Magnitudes measured in each filter are shifted relative to each other. Error bars are one sigma.

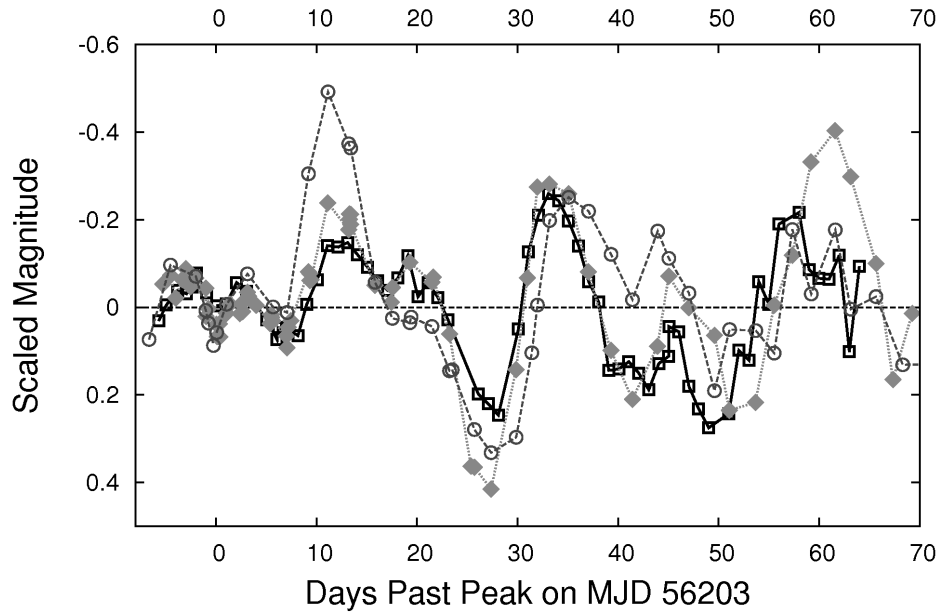


Fig. 3.— De-trended magnitudes for the V (dark open squares + solid line), U (gray shaded diamonds + dotted line), and m2 (open circles + dashed line) plotted on the same scale to highlight the differing amplitudes and relative lag of the fluctuations as a function of wavelength.

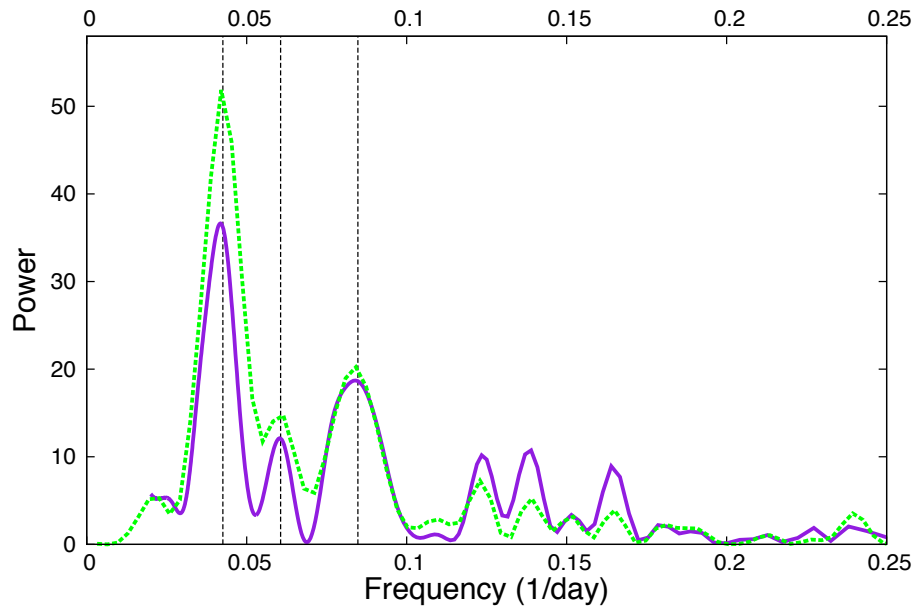


Fig. 4.— A power spectrum of the de-trended data. The dashed line is a spectrum of the full dataset. The solid line is the spectrum of the data excluding measurements between day $t = +20$ and $t = +40$.

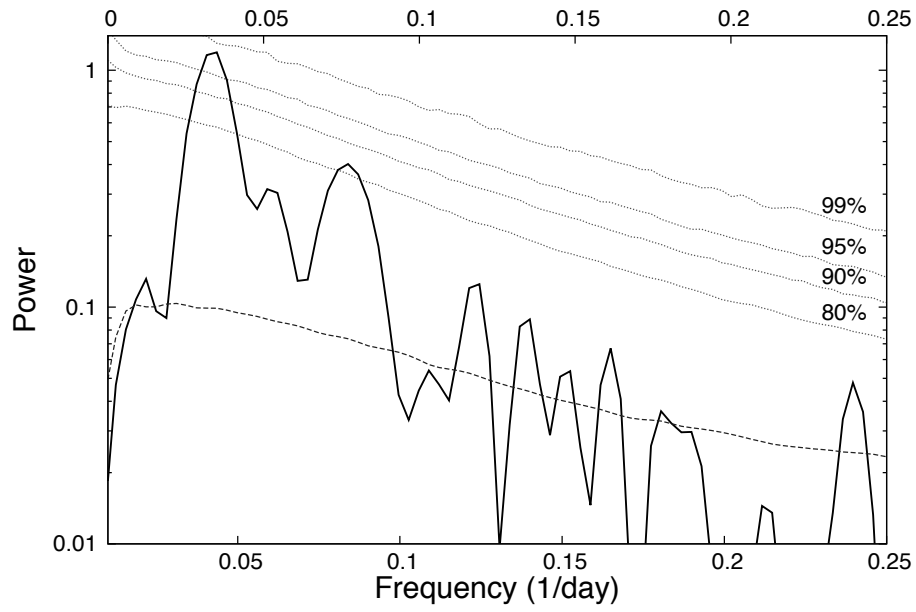


Fig. 5.— A power spectrum of the the de-trended data between day $t = +20$ and $t = +40$ (solid line) compared with an AR1 red-noise simulation (Schulz & Mudelsee 2002) (dashed line). The dotted lines depict the increasing levels of confidence calculated using a Monte-Carlo simulation with $N = 10^4$. Spectrum above the 95% confidence level has a less than 5% chance of being a false alarm.

Table 1. V Magnitudes After $t = +10$ days

Telescope	Date (MJD)	V (mag)
Hamsch	56213.08	13.798±0.055
Hamsch	56214.08	13.800±0.050
Hamsch	56215.17	13.858±0.062
Hamsch	56216.09	13.894±0.055
Hamsch	56217.09	13.972±0.055
Hamsch	56218.09	14.051±0.048
Hamsch	56219.09	14.132±0.055
Hamsch	56220.09	14.204±0.060
Hamsch	56221.09	14.226±0.048
Hamsch	56222.09	14.225±0.055
Hamsch	56223.09	14.369±0.063
Hamsch	56224.09	14.387±0.083
Hamsch	56225.09	14.471±0.061
Hamsch	56226.09	14.572±0.042
Hamsch	56229.09	14.891±0.060
Hamsch	56230.09	14.963±0.077
Hamsch	56231.09	15.038±0.100
Hamsch	56233.09	14.941±0.063
Hamsch	56234.09	14.814±0.049
Hamsch	56235.09	14.780±0.051
Hamsch	56236.09	14.780±0.048
Hamsch	56237.08	14.846±0.075
Hamsch	56238.08	14.941±0.052
Hamsch	56239.08	15.048±0.054
Hamsch	56240.08	15.178±0.053
Hamsch	56241.07	15.274±0.047
Hamsch	56242.07	15.479±0.054
Hamsch	56243.07	15.525±0.054
Hamsch	56244.07	15.557±0.072
Hamsch	56245.06	15.632±0.062
Hamsch	56246.06	15.719±0.058
Hamsch	56247.06	15.708±0.059
Barber	56248.04	15.739±0.034
Hamsch	56248.05	15.672±0.081
Hamsch	56249.05	15.733±0.047
Hamsch	56250.05	15.906±0.064
Hamsch	56251.02	16.005±0.108
Hamsch	56252.02	16.097±0.185
Hamsch	56254.02	16.162±0.086
Hamsch	56255.02	16.066±0.081
Hamsch	56256.02	16.138±0.106
Hamsch	56257.00	16.005±0.065
Hamsch	56258.00	16.106±0.059
Hamsch	56259.01	15.971±0.081
Hamsch	56261.00	16.041±0.073

Table 1—Continued

Telescope	Date (MJD)	V (mag)
Hamsch	56262.01	16.220±0.071
Hamsch	56263.01	16.288±0.058
Hamsch	56264.00	16.338±0.067
Hamsch	56265.01	16.332±0.064
Hamsch	56266.01	16.600±0.100
Hamsch	56267.01	16.453±0.086

Table 2. Parameters For Light Curve Fits

Filter	a_1 (mag)	$b_1 \times 10^2$ (mag/day)	$c_1 \times 10^3$ (mag/day ²)	N	χ^2 x100	a_2 (mag)	$b_2 \times 10^2$ (mag/day)	$c_2 \times 10^3$ (mag/day ²)	N	χ^2 x100	a_3 (mag)	$b_3 \times 10^2$ (mag/Log(day))	N	χ^2 x100
Ic	13.81±0.02	-5.5±0.5	3.5±0.5	18	0.48	13.02±0.14	5.5±1.1	^a	34	1.54	10.71±0.17	1.14±0.05	35	2.12
Rc	13.76±0.01	-5.2±0.2	6.2±0.4	5	0.02	13.22±0.05	4.8±0.2	^a	24	0.92	10.80±0.26	1.17±0.08	24	3.43
V	13.86±0.02	-6.6±0.3	7.9±0.7	16	0.35	13.36±0.07	5.3±0.5	^a	55	2.07	11.33±0.21	1.13±0.06	56	12.07
B	13.90±0.02	-6.4±0.3	8.7±0.7	25	0.52	13.62±0.19	4.5±1.0	0.3±0.1	29	3.96	7.07±0.58	2.53±0.16	30	21.19
U	12.91±0.02	-5.5±0.3	8.1±0.5	35	0.45	12.15±0.15	9.3±0.9	^a	37	4.41	5.10±0.43	3.03±0.12	38	19.40
w1	12.25±0.02	-3.3±0.4	9.5±0.8	13	0.39	11.48±0.17	15.0±0.9	-0.6±0.1	28	2.61	3.70±0.37	3.53±0.10	29	7.29
m2	12.09±0.03	-2.7±0.6	9.6±1.0	9	0.60	10.97±0.13	19.6±0.6	-1.0±0.1	35	3.39	3.05±0.24	3.86±0.07	36	5.03
w2	12.18±0.02	-1.8±0.3	10.3±0.6	23	0.38	11.01±0.15	21.7±0.9	-1.3±0.1	37	3.92	3.62±0.17	3.80±0.05	38	2.77

^aThe fit for this term was consistent with zero.

Note. — These are the best fit parameters to the measured brightness in each band for the time periods $-8 < t < +10$ days (brightness = $a_1 + b_1 t + c_1 t^2$) and $+10 < t < 75$ days (brightness = $a_2 + b_2 t + c_2 t^2$). For comparison, the fit parameters and χ^2 for brightness = $a_3 + b_3 \text{Log}(t)$ to $+10 < t < 75$ days are also included.